In Vivo Results of a New Focal Tissue Ablation Technique: Irreversible Electroporation

Jon F. Edd* , *Student Member, IEEE*, Liana Horowitz, Rafael V. Davalos, Lluis M. Mir, and Boris Rubinsky

***Abstract*—This paper reports results of *in vivo* experiments that confirm the feasibility of a new minimally invasive method for tissue ablation, irreversible electroporation (IRE). Electroporation is the generation of a destabilizing electric potential across biological membranes that causes the formation of nanoscale defects in the lipid bilayer. In IRE, these defects are permanent and lead to cell death. This paper builds on our earlier theoretical work and demonstrates that IRE can become an effective method for nonthermal tissue ablation requiring no drugs. To test the capability of IRE pulses to ablate tissue in a controlled fashion, we subjected the livers of male Sprague-Dawley rats to a single 20-ms-long square pulse of 1000 V/cm, which calculations had predicted would cause nonthermal IRE. Three hours after the pulse, treated areas in perfusion-fixed livers exhibited microvascular occlusion, endothelial cell necrosis, and diapedeses, resulting in ischemic damage to parenchyma and massive pooling of erythrocytes in sinusoids. However, large blood vessel architecture was preserved. Hepatocytes displayed blurred cell borders, pale eosinophilic cytoplasm, variable pyknosis and vacuolar degeneration. Mathematical analysis indicates that this damage was primarily nonthermal in nature and that sharp borders between affected and unaffected regions corresponded to electric fields of 300–500 V/cm.**

***Index Terms*—Bioheat equation, cancer therapy, electro-permeabilization, finite element analysis, microvascular occlusion.**

I. Introduction

FOCAL tissue ablation, the destruction of undesirable tissues in a controlled and focused way while sparing the surrounding healthy tissue, has become an important minimally invasive surgical alternative to resection surgery for the treatment of benign or malignant tumors. Several methods for tissue ablation elevate the temperature of the tissue to induce cell necrosis. These thermal methods include radio frequency ablation (RF) [1], high-intensity focused ultrasound [2] and interstitial laser photocoagulation [3]. Most electrical methods rely on resistive heating (the Joule effect) to elevate the temperature of the targeted tissue. For example, RF ablation requires an active electrode to be introduced into the undesirable tissue for the application of a large oscillating voltage (up to 4 kV at frequencies as high as 500 kHz) which heats the tissue to coagulation. A recent review of these and other thermal techniques applied to liver cancer, such as simple Joule heating [4] and microwave ablation [5], gives a thorough analysis of each [6].

This paper explores a new technique for minimally invasive tissue ablation with electrical pulses: irreversible electroporation (IRE). Electroporation is a technique, commonly used in biotechnology and medicine, in which short (microsecond to millisecond) high voltage pulses are applied (via contact electrodes) to cells or tissues for the purpose of permeabilizing the cell membranes. It has been determined from observations of species transport across cell membranes [7] and measurements determining the change in membrane electrical properties after pulsing [8]–[11] that electroporation allows normally impermeant matter to diffuse more freely through the membranes [12]. This altered behavior of cell membranes was first reported in the mid 1960's [13]. A subsequent study showed that certain electrical pulses can kill micro-organisms through the phenomenon now known as "irreversible electroporation" [14]. The increased permeability of the cell membrane due to an induced electric field was first recognized in the early 1970s [7], [15], [16]. The ability of the membrane to reseal, in what is now known as "reversible electroporation," was discovered during the late 1970s [17]–[19]. These studies have led to the understanding that when the electric potential across the cell membranes increases due to the high voltage pulse, the cell membrane can either be: 1) not permeabilized; 2) permeabilized reversibly and temporarily; or 3) permeabilized irreversibly, in which case the cell will subsequently become necrotic. Although the mechanism through which electrical pulses permeabilize the cell membrane is not yet fully understood, the outcome depends on pulse amplitude, duration, number of pulses and the frequency of repetition. It is thought that the induced potential across the cell membrane causes instabilities in the polarized lipid bilayer. The unstable membrane then alters its shape forming aqueous pathways that possibly are nano-scale pores through the membrane, hence the name *electroporation* [12], [20], [21].

Though reversible electroporation has been used for decades [7], [13], [15], [16], [18], [22]–[25] and IRE has been known to occur for many years [14], no reported results analyze the efficacy of IRE as an independent tissue ablation method. Therefore, the first goal of this paper was to test this with *in vivo* experiments. Recently, we reported in a mathematical study that,

Manuscript received August 7, 2005; revised January 22, 2006. This work was supported in part by the National Institutes of Health (NIH) under Grant 5R01RR1459. *Asterisk indicates corresponding author.*

*J. F. Edd is with the Department of Mechanical Engineering, University of California, Berkeley, CA 94720 USA (e-mail: jonedd@me.berkeley.edu).

L. Horowitz is with the Department of Mechanical Engineering, University of California, Berkeley, CA 94720 USA.

R. V. Davalos is with the Microsystems Division at Sandia National Laboratories, Livermore, CA 94550 USA (e-mail: rvdaval@sandia.gov).

L. M. Mir is with the UMR 8121 CNRS, Institute Gustave-Roussy, 94805 Villejuif, France (e-mail: luismir@igr.fr).

B. Rubinsky is with the Departments of Bioengineering and Mechanical Engineering, University of California, Berkeley, CA 94720 USA (e-mail: rubinsky@me.berkeley.edu).

Digital Object Identifier 10.1109/TBME.2006.873745

0018-9294/$20.00 © 2006 IEEE

although dc pulses cause Joule heating, IRE could be used as a nonthermal treatment for cancer [26]. That analysis predicted that a domain of electrical pulses could be found in which IRE alone was the cause of tissue ablation (thermal effects negligible). This distinction is important because other methods of ablation are applied in a similar manner (through electrodes) and can even cause some of the same effects, though superimposed upon the primary thermal effect. The reason that our pulses are able to cause IRE and not thermal ablation is due to their relatively small energy input into the system. Consequently, the second goal of this paper was to verify experimentally that it is possible to ablate substantial volumes of tissue with IRE alone. If this were possible, it would mean the validation of a new method of focal tissue ablation that does not require drugs, in contrast with electrochemotherapy, a cancer treatment which works to focus drug uptake by increasing the permeability of cells, in areas treated with reversible electroporation pulses, to therapeutic molecules [25]. In order to test this, it was necessary to conduct an *in vivo* study that correlated the electric field and temperature distributions with the resulting effects on the treated tissue.

II. Materials and Methods

A. Animals

Male Sprague-Dawley rats (250–350 g) were obtained from Charles River Labs through the Office of Laboratory Animal Care at the University of California, Berkeley. They received humane care from a properly trained professional in compliance with both the *Principals of Laboratory Animal Care* and the *Guide for the Care and Use of Laboratory Animals*, prepared and formulated by the Institute of Laboratory Animal Resources and published by the NIH.

B. Experimental Procedure

The experiment performed identically on each of four rats started with anesthetization of the animal via intraperitoneal injection of Nembutal solution (50 mg/ml sodium pentobarbital, *Abbott Labs*, North Chicago, IL) for a total of 100 mg sodium pentobarbital per kg of rat. Thirty minutes later, the liver was exposed via midline incision. The electrodes were then attached across one lobe of liver with the device illustrated in Fig. 1. The electrodes were made of sintered Ag/AgCl and have a 10-mm diameter and a 1-mm thickness (E255, *In Vivo Metric*, Healdsburg, CA). After measuring the frequency-dependent impedance between the electrodes for 1 min, a square pulse of 400 V was applied with a pulse generator (ECM 830, *Harvard Apparatus*; Holliston, MA) across the 4-mm gap between the electrodes for 20 ms (approximately 1 h after anesthetization). The impedance was then measured again for 1 min and the animal was observed continuously while in thermal incubation until 3 h after pulsing. At this point, the animal was euthanized.

C. Liver Histology

To fix the liver at its current state for microscopic viewing, we flushed the vasculature with physiological saline for 10 min at a hydrostatic pressure of 80 mmHg from an elevated IV drip. This was accomplished by injecting the fluid into the left ventricle and letting it exit from a cut made in the right atrium. Immediately following saline perfusion, a 5% formaldehyde fixative was perfused in the same way for 10 min. The treated liver lobe was then removed and stored in the same formaldehyde solution. Hematoxylin-eosin staining was then performed on cross sections through the center of the treated region to elucidate the morphology.

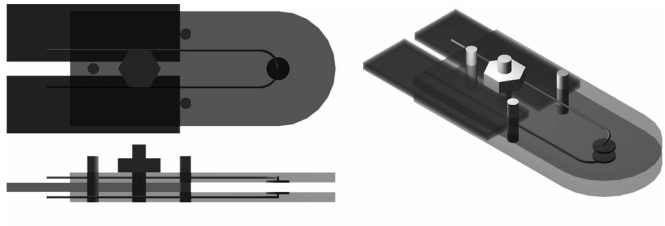

Fig. 1. Electroporation and impedance measurement device. Exposed liver lobe was placed between the two plate electrodes (10-mm diameter). Electrodes and insulating plates were held 4 mm apart by spacers inserted between the plates. Three pins that extended through both plates ensured concentricity of the electrodes (not to scale).

D. Electrical Conductivity Measurement

Simulations were then performed which incorporated the measured liver conductivity, computed in the following manner. The complex impedance of the tissue between the electrodes in the device (Fig. 1) was measured by applying several small sine-wave voltages (3 Hz to 25 kHz consecutively) across the electrodes and synchronously detecting the applied voltage and induced current waveforms (measured from voltage differences between both driving electrodes and across a resistor in the current path, respectively). The sine-wave generation and simultaneous current/voltage measurements were controlled in software (Labview 6.1, *National Instruments*, Austin, TX) that interfaced with the measurement circuit through a data acquisition card (*National Instruments*, 6071E). The magnitude of the complex impedance (Z) was then determined from Ohm's law $(Z = V/I)$. We then estimated the magnitude of the complex conductivity (σ) from $\kappa_{\mathrm{cell}} = \sigma Z$where κ_{cell} is the cell constant of the system (calculated to be 37 m^{-1} from the electrical model). This conductivity is the value we used in the thermal model to compute the temperature rise due to Joule heating $(\sigma E^2 t = \rho_m c_p \Delta T)$where E is electric field strength, t is pulse duration, $\rho_m = 1.05\,\mathrm{g/cm}^3$ is mass density, $c_p = 3600\,\mathrm{J/kgK}$ is specific heat, and ΔT is the temperature rise. The property values (except for σ) were taken from data on *in vivo* rat liver [27].

E. Electric Field Simulation

To correlate the changes observed in liver with the characteristics of the applied pulse, we simulated the electric field distribution, which determines whether or not electroporation occurs [28], with a representative finite-element model. Specifically, we simulated the electric field distribution resulting from the pulse by solving for the electric potential (ϕ) that obeys the Laplace equation

$$\nabla \cdot (\sigma \nabla \phi) = 0. \tag{1}$$

This was performed with a commercial finite element package (FEMLab, *Comsol AS*, Stockholm, Sweden). The liver was modeled as a cylindrically symmetric disk of 2 cm diameter and 4-mm thickness with concentric electrodes of 1 cm diameter on either side of the liver. The potential on the liver surface adjacent to the top electrode was taken to be 400 V and that touching the bottom electrode was grounded. The remaining surfaces were treated as electrically insulating. The assumed uniform and isotropic conductivity value of 0.05 S/m, in aggreement with published data, was taken from impedance measurements made on the liver immediately prior to pulsing at a signal frequency of 3 Hz (which lies near the center of the power spectrum for a 20 ms square pulse).

F. Temperature Field Simulation

Similarly, we computed the elevated temperature field during the pulse, resulting from Joule heating, to determine what role thermal ablation played in the macroscopically visible changes. This was possible once the electric field distribution was calculated. Specifically, the temperature field was computed at times during the pulse from similar numerical solution of the Pennes bioheat equation [29]

$$\nabla \cdot (k\nabla T) + w_b c_b (T_a - T) + q_m + q_e = \rho_m c_p \frac{\partial T}{\partial t} \qquad (2)$$

with the addition of a Joule heating term ($q_e = \sigma|\nabla\phi|^2$). Here, ($k$) is thermal conductivity of the tissue, (w_b) is the blood perfusion rate, (c_b) is the specific heat of the blood, $T_a = 37°\mathrm{C}$ is the arterial temperature, (q_m) is the metabolic heat generation, (ρ_m) is the mass density of the tissue, and (c_p) is the specific heat of the tissue (property values were taken from [27], [30]). The boundary conditions were all insulating and the initial condition was 37 °C everywhere. Each simulation was performed with a modified implementation of the axisymmetric heat transfer module in FEMLab with a mesh of approximately 2×10^4 biquadratic triangular elements.

III. Results and Discussion

A. Macroscopic Analysis

The results described in this section were obtained from identical experiments on four rats. The cross sections of each treated liver (held at 4-mm thickness) showed a well defined treated region that corresponded to the dark brown color in the associated photographs in Fig. 2(a). These regions corresponded to a failure of the employed perfusion-fixation technique to remove erythrocytes, indicating that the treatment had caused macroscopic vascular disruption and a resultant pooling of blood. The associated nondeformed cross sections from H&E histology in Fig. 2(b) also showed clear margination of treated and nontreated areas. In the central treated regions, widespread but variable congestion in the small to medium blood vessels and surrounding parenchyma was evident. Large blood vessels were free from entrapped erythrocytes in most cases, indicating that the perfusion-fixation in formalin had been able to push through these vessels. The parenchyma in treated regions also showed

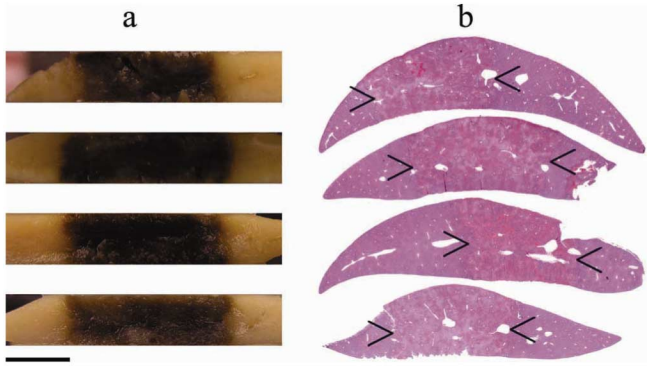

Fig. 2. Cross sections of pulsed livers fixed for viewing 3 h after pulsing. (a) Photographs of each of four treated livers taken at the central plane of the treated region. Dark brown areas correspond to macroscopic pooling of erythrocytes while pale regions indicate successful perfusion of saline followed by formaldehyde, resulting in removal of erythrocytes. The livers were held between two plates 4 mm apart to recreate the geometry that was present during the pulse. (b) Corresponding scans of histology slices taken along the same plane. Arrows designate the extent of the treated region which exhibits variable pale eosinophilia and widespread congestion as compared to the normal parenchyma (affected areas had cross-sectional areas of 51.3, 59.6, 48.6, and 49.9 mm^2 from top to bottom). Bar indicates 5 mm in all photos. (Color version available online at http://ieeexplore.ieee.org.)

variations in color which seemed to correspond partly to lobular structure. Centrilobular regions were darker in most cases, while other areas in the treated region were paler in color than even the untreated regions. The range and mean of the cross-sectional areas of the affected regions in Fig. 2(b) were 48.6–59.6 and 52.4 mm^2, respectively. This indicated an area of treatment with a slightly larger cross section than the cylinder of tissue between the electrodes (4 mm × 10 mm).

B. Electric and Temperature Fields

The computed cylindrically symmetric electric field distribution has been superimposed upon the cross section of the last treated liver in Fig. 3(b). Previous studies in muscle have estimated thresholds for reversible electroporation (eight pulses, 1 Hz) at 450 V/cm for 100 μs [31] and 200 V/cm for 20 ms [32]. We also know that the threshold for IRE in liver for 100 μs pulses has been reported as 637 ± 43 V/cm (eight pulses at 1 Hz) [33]. So we should have expected that in our case (only one pulse of 20 ms) the threshold for IRE would have been 300 V/cm or greater. Indeed, this was consistent with Fig. 3(b) which showed the transition to be 300–500 V/cm. Throughout most of the treated area, field strength was very uniform at 900–1100 V/cm. It was for this characteristic that we chose to apply the pulse in a parallel-plate configuration. However, small annular zones with electric fields exceeding 2000 V/cm existed near the edges of the electrode contact area. In the most severe of these areas, tissue was ablated thermally. This can be seen from Fig. 3(a) as a thin semicircular arc of discolored tissue. Nevertheless, the temperature rise in the majority of the treated region was 2 °C to 3 °C [Fig. 3(c)]. However, since the prepulse conductivity was used for the thermal model, the fact that tissue conductivity increases during an electroporation pulse [34], [35] means that the true temperature rise was somewhat higher. From postpulse conductivity measurement, we determined that the conductivity increase due to the pulse was between 15.6% and 26.3% at 3 Hz

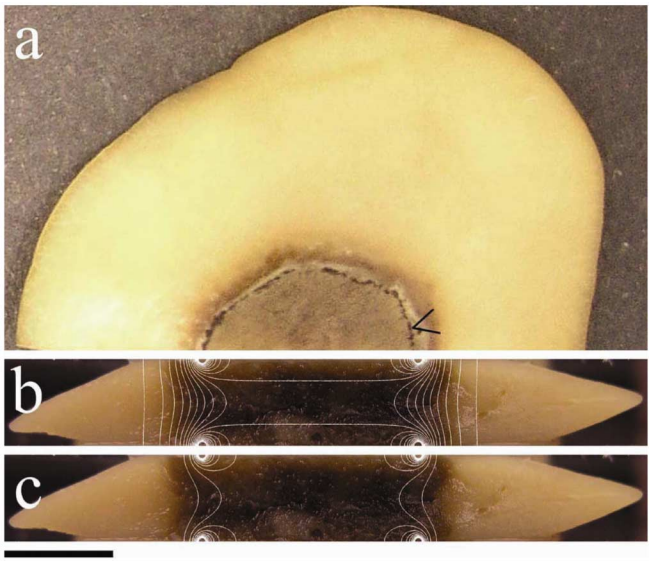

Fig. 3. Computed electric field strength during the pulse and resulting temperature rise. (a) Top view of the last liver from Fig. 2(a). Thin semicircle of thermally ablated tissue is visible near the extents of the tissue ablated by IRE. (b) Electric field strength resulting from the 400 V pulse. Lines of constant electric field strength are superimposed upon the side view of this liver. The lines represent 100 V/cm increments from 100 V/cm to 2000 V/cmwhere the lowest values are at the far left and right edges and the highest occur within an annular region corresponding to the semicircle referred to in the top view. Two lines that cross the central region are 1000 V/cm contours. (c) Temperature rise due to Joule heating at the end of the 20 ms pulse. Lines of constant temperature are superimposed upon the same side view. The contours represent 1 °C increments from 38 °C to 50 °C where the lowest values are at the far left and right edges (ΔT is proportional to the square of the local electric field strength). The annular region where temperatures exceed 50 °C corresponds to the area that experienced thermal ablation (arrow), while the remaining effects were nonthermal in nature. Bar indicates 5 mm in all photos. (Color version available online at http://ieeexplore.ieee.org.)

with a mean of 24.9%. The conductivity rise during the pulse could be somewhat higher, so the joule heating, linearly related to conductivity, could be more than 25% higher than the predicted values towards the end of the pulse. Still, we concluded that the observed macroscopic changes in all areas except the annular region of high current density (about 0.6 mm wide) were nonthermal in nature and must have been caused by the electric field strength alone [26].

C. Microscopic Analysis

Histological analysis revealed acute damage to the tissue in treated regions. In central treated areas, widespread pale eosinophilia and congestion in the sinusoids was evident. In some areas [Fig. 4(a)] this congestion was so dense as to suggest the intercellular adhesion between adjacent hepatocytes had been impaired. Massive diapedeses and early fibrin deposition also occured within the sinusoids. These conditions would likely have caused coagulative necrosis of the hepatocytes. Additionally, vacuolar degeneration of hepatocytes was present throughout the central treated region, but occurred most significantly in centrilobular areas, further suggesting an interruption of blood flow and oxygen supply which resulted in ischemic damage.

At the margins of treated areas [Fig. 4(b)–(d)], various stages of cellular degeneration were present. In all cases, the treated side exhibited pale eosinophilic cytoplasm when compared with the untreated side. In some areas [Fig. 4(c)], moderate pyknosis of the nuclei and sinusoidal congestion were present in the treated side and conspicuously absent in the other side. Cell borders were also clearly visible on the nontreated side and nearly indistinguishable in the treated side [Fig. 4(d)]. This suggests that the primary expected consequence of the procedure had occurred: cell membrane disruption. In other areas [Fig. 4(d)], obvious vacuolar degeneration marked the boundary between healthy and pathological parenchyma. As noted in previous studies of reversible electroporation [36], the line of demarcation was often surprisingly narrow (between adjacent hepatocytes), but did not correspond to lobular boundaries.

Throughout the treated area, insult to endothelial cells was evident. In nearly all cases [Fig. 4(e)–(l)], endothelial necrosis was present and large numbers of neutrophils were marginated along and had infiltrated within the vessel walls, indicating acute vascular inflammation. Erythrocytes were also seen pooling immediately beneath the endothelium [Fig. 4(f)–(j)]. Notably, at 3 h after treatment, this vascular necrosis had not destroyed large blood vessel architecture as indicated by the successful flushing of blood from these vessels (clear lumen). Only occasional large blood vessels showed interrupted blood flow and occlusion with red blood cells and fibrin deposition [Fig. 4(e)]; however, many contained an early organized attached thrombus [Fig. 4(f)].

IV. Conclusion

Because of the lines of demarcation between treated areas and normal areas, the affected area is similar to a per-acute infarct before morphologic changes indicative of necrosis occur. This is further substantiated by the congestion solely in the treated area. The likely pathogenesis of the treatment is that there was a field effect of IRE which caused membrane disruption, pale eosinophilia, variable pyknosis and vacuolar degeneration of hepatocytes. Superimposed upon this effect was a pulse-mediated necrosis of endothelial cells causing vascular compromise, thrombus formation and diapedeses, resulting in a widespread but predominantly centrilobular sinusoidal congestion and vacuolar degeneration.

Previous studies on rabbit liver tumors with needle electrodes (several 100 μs pulses of 850-V/cm voltage-to-distance ratio) have noted many similar effects [37], albeit in the reversible range. They reported a transient vascular lock (observed externally for 15–20 min) and suspected enhanced vascular permeability. Moreover, the regions that were ablated in this study were limited to the locations very close to the needles. This vascular lock, induced by dc pulses in the reversible range, was also observed in studies on mouse muscle as a delayed (1–2 min) perfusion of injected dye [38] and a 30% normal blood flow rate at 1 h after pulsing in mouse fibrosarcoma [39]. Some studies have noted that electroporation-mediated incorporation of genes into endothelial cells has little effect on the response of the vessel to stimuli [40], while others have noted varying degrees of temporary blood flow reduction due to electrochemotherapy [41],

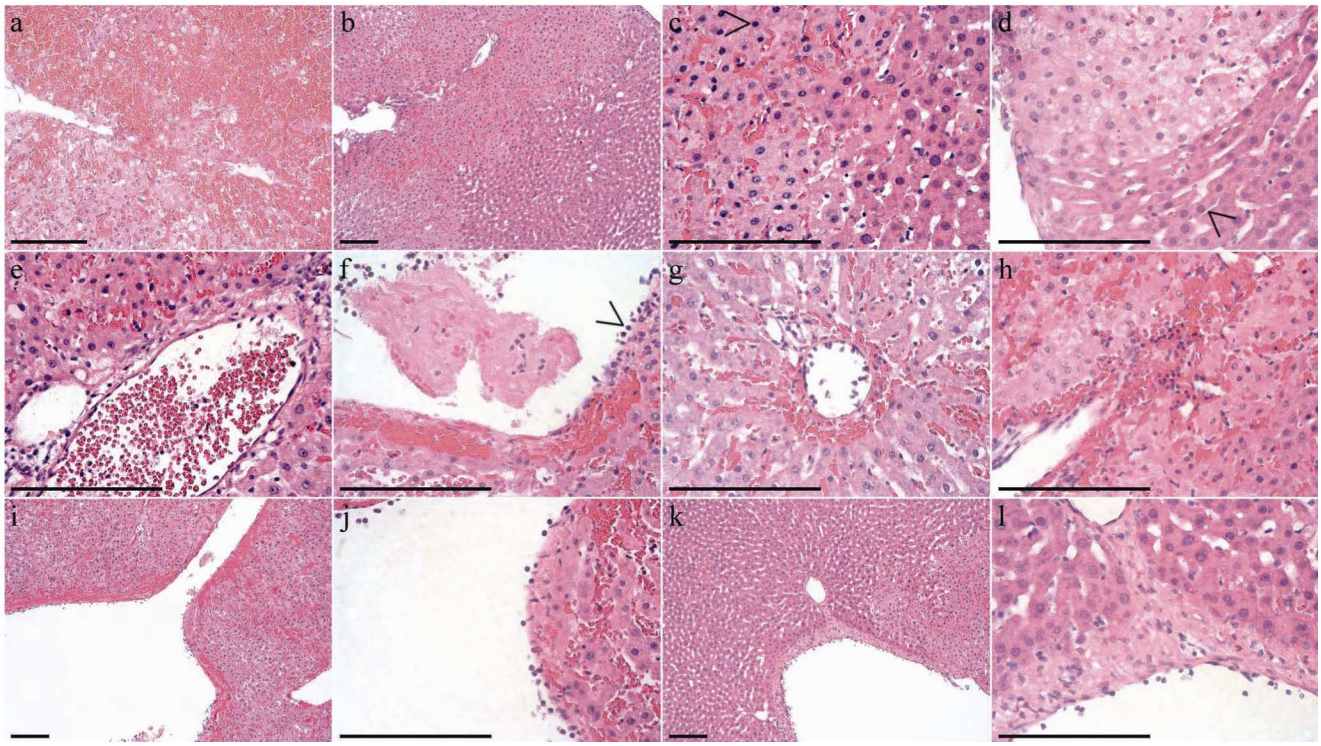

Fig. 4. Microscopic viewing of slides in Fig. 2(b). (a) Central treated area showing widespread pale eosinophilia and sinusoidal congestion. (b) Border of treated area. (c) Border showing pyknosis of nuclei, pale eosinophilia, congestion, indistinguishable cell borders and mild vacuolar degeneration in the treated (left) side but not in the unaffected (right) side. Arrow indicates pyknotic nucleus (treated). (d) Pale eosinophilia and vacuolar degeneration of hepatocytes at the border. Transition zone is very sharp (between adjacent hepatocytes). Arrow indicates evident cell borders (untreated). (e) Complete occlusion of large blood vessel and fibrin deposition in the lumen. (f) Early organized attached thrombus with entrapped neutrophils and erythrocytes. Acute congestion and inflammation in the endothelium is present and substantiated by neutrophilic infiltrates (arrow). (g)–(j) Vascular inflammation and diapedeses. (k)–(l) Shunting of current between blood vessels. Pale eosinophilic area defines a narrow path of current flow from one low resistance area to another, which resulted in necrosis due to the high current densities incurred locally. Bars indicate 150 μm in all photos. (Color version available online at http://ieeexplore.ieee.org.)

[42], some even showing complete shutdown 24 h after electrochemotherapy [43]. However, these studies investigated reversible electroporation alone or in combination with nonpermeant cytotoxic drugs (e.g., electrochemotherapy, in which case the electric pulses enhanced the cytotoxic effects of the anticancer drugs and were also responsible for the lasting antivascular effects). Further, the novelty of this study in relation to the effects on blood flow is that we see widespread sinusoidal occlusion at 3 h after pulsing and without drugs.

The goal of this paper was to evaluate the effects of IRE pulses *in vivo*. The results suggest that IRE can be used to nonthermally ablate large volumes of tissue in a controlled manner with a sharp boundary between affected and unaffected tissues. It is very simple, involving the application of minimally invasive electrodes very similar to radiofrequency ablation [1], [4], but is much faster (microseconds-milliseconds as compared with minutes-hours) and more precise as it does not depend on blood flow. More importantly, it does not require any drugs. Notably, it has been shown to be especially effective in causing widespread endothelial necrosis and congestion in the treated region, causing any tissues that may survive the pulse itself to face ischemia and coagulation as well. This treatment could also allow the instantaneous local entrapment in the sinusoids of any chemicals such as drugs or imaging markers that are perfused through the tissue before and during the electroporation pulse, enabling imaging of the extents of the treated region and also a synergistic effect with chemotherapy. As this paper has shown, IRE can provide a new complementary weapon against cancer in the armament of medicine.

ACKNOWLEDGMENT

The authors would like to acknowledge Oncobionic for supplying the pulse generator, Dr. Stephen M. Griffey for help with histopathology and Kyle Yeates for construction of the electroporation device (Fig. 1).

REFERENCES

[1] L. W. Organ, "Electrophysiological principles of radiofrequency lesion making," *Appl. Neurophysiol.*, vol. 39, pp. 69–76, 1976.
[2] R. Yang, N. T. Sanghvi, F. J. Rescorla, K. K. Kopecky, and J. L. Grosfeld, "Liver cancer ablation with extracorporeal high-intensity focused ultrasound," *Eur. Urol.*, vol. 23, pp. 17–22, 1993.
[3] D. Hashimoto, M. Takami, and Y. Idezuki, "In-depth radiation therapy by yttrium-aluminum-garnet laser for malignant tumors in the liver under ultrasonic imaging," *Gastroenterology*, vol. 88, p. 1663, 1985.
[4] A. Erez and A. Shitzer, "Controlled destruction and temperature distribution in biological tissue subjected to monoactive electrocoagulation," *J. Biomech. Eng.*, vol. 102, pp. 42–49, 1980.
[5] K. Tabuse, "A new operative procedure of hepatic surgery using a microwave tissue coagulator," *Nippon Geka Hokan*, vol. 48, pp. 160–172, 1979.
[6] G. Garcea, T. D. Lloyd, C. Aylott, G. Maddern, and D. P. Berry, "The emergent role of focal liver ablation techniques in the treatment of primary and secondary liver tumours," *Eur. J. Cancer*, vol. 39, pp. 2150–2164, 2003.

[7] E. Neumann and K. Rosenheck, "Permeability changes induced by electric impulses in vesicular membranes," *J. Membrane Biol.*, vol. 10, pp. 279–290, 1972.
[8] K. Kinosita, Jr and T. Y. Tsong, "Voltage-induced conductance in human erythrocyte membranes," *Biochimica et Biophysica Acta*, vol. 554, pp. 479–497, 1979.
[9] Y. Huang and B. Rubinsky, "Microfabricated electroporation chip for single cell membrane permeabilization," *Sensors Actuators A (Physical)*, vol. A89, pp. 242–249, 2001.
[10] L. V. Chernomordik, S. I. Sukharev, S. V. Popov, V. F. Pastushenko, A. V. Sokirko, I. G. Abidor, and Y. A. Chizmadzhev, "The electrical breakdown of cell and lipid membranes: the similarity of phenomenologies," *Biochimica et Biophysica Acta*, vol. 902, pp. 360–373, 1987.
[11] M. Hibino, M. Shigemori, H. Itoh, K. Nagayama, and K. Kinosita, "Membrane conductance of an electroporated cell analyzed by submicrosecond imaging of transmembrane potential," *Biophys. J.*, vol. 59, pp. 209–220, 1991.
[12] J. C. Weaver and Y. A. Chizmadzhev, "Theory of electroporation: a review," *Bioelectrochem. Bioenergetics*, vol. 41, pp. 135–160, 1996.
[13] H. G. A. Coster, "Quantitative analysis of the voltage-current relationship of fixed charge membranes and the assosciated property of 'punch-through'," *Biophysical J.*, vol. 5, pp. 669–686, 1965.
[14] A. J. Sale and W. A. Hamilton, "Effects of high electric fields on microorganisms 1: killing of bacteria and yeasts," *Biochimica et Biophysica Acta*, vol. 148, pp. 781–788, 1967.
[15] J. M. Crowley, "Electrical breakdown of biomolecular lipid membranes as an electromechanical instability," *Biophysical J.*, vol. 13, pp. 711–724, 1973.
[16] U. Zimmermann, J. Vienken, and G. Pilwat, "Dielectric breakdown of cell membranes," *Biophysical J.*, vol. 14, pp. 881–899, 1974.
[17] K. Kinosita, Jr and T. Y. Tsong, "Hemolysis of human erythrocytes by a transient electric field," *Proc. Nat. Acad. Sci. USA*, vol. 74, pp. 1923–1927, 1977.
[18] P. F. Baker and D. E. Knight, "Calcium-dependent exocytosis in bovine adrenal medullary cells with leaky plasma membranes," *Nature*, vol. 276, pp. 620–622, 1978.
[19] B. Gauger and F. W. Bentrup, "A study of dielectric membrane breakdown in the fucus egg," *J. Membrane Biol.*, vol. 48, pp. 249–264, 1979.
[20] D. C. Chang, B. M. Chassy, J. A. Saunders, and A. E. Sowers, *Guide to Electroporation and Electrofusion*. San Diego, CA: Academic, 1992.
[21] M. Tarek, "Membrane electroporation: a molecular dynamics simulation," *Biophysical J.*, vol. 88, pp. 4045–4053, 2005.
[22] L. M. Mir, M. Belehradek, C. Domenge, B. Luboniski, S. Orlowski, J. Belehradek, B. Schwaab, B. Luboniski, and C. Paoletti, "Electrochemotherapy, a novel antitumor treatment: first clinical trial," *Comptes Rendus de l'Academie des Sciences Serie III Sciences de la Vie*, vol. 313, pp. 613–618, 1991.
[23] L. M. Mir, S. Orlowski, J. Belehradek, Jr., and C. Paoletti, "Electrochemotherapy potentiation of antitumour effect of bleomycin by local electric pulses," *Eur. J. Cancer*, vol. 27, pp. 68–72, 1991.
[24] S. B. Dev, D. P. Rabussay, G. Widera, and G. A. Hofmann, "Medical applications of electroporation," *IEEE Trans. Plasma Sci.*, vol. 28, no. 1, pp. 206–223, Feb. 2000.
[25] L. M. Mir, "Therapeutic perspectives of *in vivo* cell electropermeabilization," *Bioelectrochemistry*, vol. 53, pp. 1–10, 2000.
[26] R. V. Davalos, L. M. Mir, and B. Rubinsky, "Tissue ablation with irreversible electroporation," *Ann. Biomed. Eng.*, vol. 33, pp. 223–231, 2005.
[27] F. A. Duck, *Physical Properties of Tissue: A Comprehensive Reference Book*. San Diego, CA: Academic, 1990.
[28] D. Miklavcic, K. Beravs, D. Semrov, M. Cemazar, F. Demsar, and G. Sersa, "The importance of electric field distribution for effective *in vivo* electroporation of tissues," *Biophysical J.*, vol. 74, pp. 2152–2158, 1998.
[29] H. H. Pennes, "Analysis of tissue and arterial blood temperatures in the resting human forearm," *J. Appl. Physiol.*, vol. 1, pp. 93–122, 1948.
[30] Z.-S. Deng and J. Liu, "Blood perfusion-based model for characterizing the temperature fluctuations in living tissue," *Physica A: Statist. Mech. Applicat.*, vol. 300, pp. 521–530, 2001.
[31] J. Gehl and L. M. Mir, "Determination of optimal parameters for *in vivo* gene transfer by electroporation, using a rapid *in vivo* test for cell permeabilization," *Biochem. Biophysical Res. Commun.*, vol. 261, pp. 377–380, 1999.
[32] J. Gehl, T. H. Sorensen, K. Nielsen, P. Raskmark, S. L. Nielsen, T. Skovsgaard, and L. M. Mir, "*In vivo* electroporation of skeletal muscle: threshold, efficacy and relation to electric field distribution," *Biochimica et Biophysica Acta*, vol. 1428, pp. 233–240, 1999.
[33] D. Miklavcic, D. Semrov, H. Mekid, and L. M. Mir, "A validated model of *in vivo* electric field distribution in tissues for electrochemotherapy and for DNA electrotransfer for gene therapy," *Biochimica et Biophysica Acta*, vol. 1523, pp. 73–83, 2000.
[34] D. Sel, D. Cukjati, D. Batiuskaite, T. Slivnik, L. M. Mir, and D. Miklavcic, "Sequential finite element model of tissue electropermeabilization," *IEEE Trans. Biomed. Eng.*, vol. 52, no. 5, pp. 816–827, May 2005.
[35] N. Pavselj, Z. Bregar, D. Cukjati, D. Batiuskaite, L. M. Mir, and D. Miklavcic, "The course of tissue permeabilization studied on a mathematical model of a subcutaneous tumor in small animals," *IEEE Trans. Biomed. Eng.*, vol. 52, no. 8, pp. 1373–1381, Aug. 2005.
[36] J. Belehradek, Jr., S. Orlowski, L. H. Ramirez, G. Pron, B. Poddevin, and L. M. Mir, "Electropermeabilization of cells in tissues assessed by the qualitative and quantitative electroloading of bleomycin," *Biochimica et Biophysica Acta*, vol. 1190, pp. 155–163, 1994.
[37] L. H. Ramirez, S. Orlowski, D. An, G. Bindoula, R. Dzodic, P. Ardouin, C. Bognel, J. Belehradek, Jr., J. N. Munck, and L. M. Mir, "Electrochemotherapy on liver tumours in rabbits," *Br. J. Cancer*, vol. 77, pp. 2104–2111, 1998.
[38] J. Gehl, T. Skovsgaard, and L. M. Mir, "Vascular reactions to *in vivo* electroporation: characterization and consequences for drug and gene delivery," *Biochimica et Biophysica Acta*, vol. 1569, pp. 51–58, 2002.
[39] G. Sersa, M. Cemazar, C. S. Parkins, and D. J. Chaplin, "Tumour blood flow changes induced by application of electric pulses," *Eur. J. Cancer*, vol. 35, pp. 672–677, 1999.
[40] J. B. Martin, J. L. Young, J. N. Benoit, and D. A. Dean, "Gene transfer to intact mesenteric arteries by electroporation," *J. Vasc. Res.*, vol. 37, pp. 372–380, 2000.
[41] T. Ivanusa, K. Beravs, M. Cemazar, V. Jevtic, F. Demsar, and G. Sersa, "MRI macromolecular contrast agents as indicators of changed tumor blood flow," *Radiol. Oncol.*, vol. 35, pp. 139–147, 2001.
[42] G. Sersa, M. Krzic, M. Sentjurc, T. Ivanusa, K. Beravs, V. Kotnik, A. Coer, H. M. Swartz, and M. Cemazar, "Reduced blood flow and oxygenation in SA-I tumours after electrochemotherapy with cisplatin," *Br. J. Cancer*, vol. 87, pp. 1047–1054, 2002.
[43] G. Sersa, M. Cemazar, and D. Miklavcic, "Tumor blood flow modifying effects of electrochemotherapy: a potential vascular targeted mechanism," *Radiol. Oncol.*, vol. 37, pp. 43–48, 2003.

Jon F. Edd (S'03) was born in Monroeville, PA, in 1978. He received the B.S. degree in mechanical engineering from the University of Texas, Austin, in 2001. He is currently working toward the Ph.D. degree at the University of California, Berkeley.

His main research interests are in electrical impedance tomography, cryosurgery, electroporation, and bioMEMS.

Liana Horowitz received the M.Sc. degree from the Hebrew University, Jerusalem, Israel, in 1978. Her thesis research was in the area of zoology.

During this project she was a Visiting Scientist with the Department of Mechanical Engineering at the University of California at Berkeley.

Rafael V. Davalos was born in Bethesda, MD, in 1972. He received the B.S. and M.S. degrees in mechanical engineering from Cornell University, Ithaca, NY, in 1994 and in 1995 from the University of California, Berkeley, in 1995, respectively. He completed the Ph.D. degree in bioengineering from the Department of Mechanical Engineering at the University of California, Berkeley, in 2002.

He is currently a Senior Member of Technical Staff in the Microsystems Division at Sandia National Laboratories, Livermore, CA. His main research interests are in image-guided surgery, *in vivo* and *in vitro* electrical manipulation of cells, BioMEMS, and microsystems.

Lluis M. Mir was born in 1954 in Barcelona, Spain. He received the B.Sc. degree from the University of Paris VI, Paris, France, in 1976, and the Ph.D. Degree from the University of Toulouse, Toulouse, France, in 1983.

He is a Fellow with the Ecole Normale Supérieure de Paris, France. He is currently Director of Research of the CNRS at the UMR 8121 CNRS-Institute Gustave-Roussy, Villejuif, France. His main interests lie in the fields of membrane electropermeabilization *in vitro* and *in vivo*, especially with regard to the transfer of antitumor drugs after tumor cells electroporation (electrochemotherapy) and to the electrotransfer of genes (electrogenetherapy) to healthy and malignant tissues. He is also Professor Adjunct, and since December 2004, Honorary Senator, of the University of Ljubljana, Slovenia.

Boris Rubinsky received the Ph.D. degree from the Massachusetts Institute of Technology, Cambridge, in 1980. His thesis research was in the area of bioengineering.

Since 1980, he is a Professor at the University of California, Berkeley. During his career, he has developed several areas of research in bioengineering, including pioneering the field of imaging monitored minimally invasive surgery in general and cryosurgery in particular. He worked on imaging technologies with ultrasound, MRI, optical imaging, and electrical imaging. He performed studies on cold tolerant and freezing tolerant animals and developed microelectromechanical bionic technology for real time interaction between electromagnetic fields and individual cells. He has published over 200 research articles and has more than 20 issued patents.